Island Arc

Island Arc (2010) **19**, 192–207

Research Article

Subduction of mantle wedge peridotites: Evidence from the Higashi-akaishi ultramafic body in the Sanbagawa metamorphic belt

KEIKO HATTORI,[1,2,*] SIMON WALLIS,[1] MASAKI ENAMI[1] AND TOMOYUKI MIZUKAMI[1,†]

[1]*Department of Earth Sciences, Nagoya University, Nagoya, 464-8602 Japan, and* [2]*Department of Earth Sciences, University of Ottawa, Ottawa, Ontario, K1N 6N5, Canada*

Abstract The Higashi-akaishi garnet-bearing ultramafic body in the Sanbagawa metamorphic belt, Southwest Japan, represents a rare example of oceanic-type ultrahigh-pressure metamorphism. The body of 2 km × 5 km is composed mostly of anhydrous dunite with volumetrically minor lenses of clinopyroxene-rich rocks. Dunite samples contain high Ir-type platinum group elements (PGE) and Cr in bulk rocks, high Mg and Ni in olivine, and high Cr in spinel. On the other hand, clinopyroxene-rich rocks contain low concentrations of Ir-type PGE and Cr, high concentrations of fluid-mobile elements in bulk rocks, and low Ni and Mg in olivine. Clinopyroxene is diopsidic with low Al_2O_3. The compositions of bulk rocks and mineral chemistry of spinel, olivine, and clinopyroxene suggest that the olivine-dominated rocks are residual mantle peridotites after high degrees of influx partial melting, and that the clinopyroxene-rich rocks are cumulates of subduction-related melts. Thus, the Higashi-akaishi ultramafic body originated from the interior of the mantle wedge, most likely the forearc upper mantle. It was then incorporated into the Sanbagawa subduction channel by a mantle flow, and underwent high pressure metamorphism to a depth greater than 100 km. Such a strong active flow in the mantle wedge is likely facilitated by the lack of serpentinites along the interface between the slab and the overlying mantle, as it was too hot for serpentine. These unusually hot conditions and strong active mantle flow may reflect conditions in the earliest stage of development of subduction, and may have been maintained by massive upwelling and subsequent eastward flow of asthenospheric mantle in the northeastern Asian continent in Cretaceous time when the Sanbagawa belt began to form.

Key words: eclogite, exhumation, garnet peridotites, mantle flow, oceanic subduction, subduction.

INTRODUCTION

The Sanbagawa metamorphic belt is an oceanic subduction-type metamorphic belt that formed along the northeastern margin of the Asian continent in late Cretaceous time (e.g. Isozaki & Itaya 1990; Wallis *et al.* 2009). Unique amongst such metamorphic belts, the Sanbagawa belt contains a large (2 km × 5 km) body of garnet-bearing peridotites: the Higashi-akaishi body (Mizukami & Wallis 2005). Small lenses of garnet-bearing peridotites have been reported from many continental collision zones, such as the Western Gneiss region of Norway, and the Dabie–Sulu orogen in China (e.g. Brueckner & Medaris 2000). However, garnet-bearing peridotite is very rare in the interior of oceanic-type subduction complexes and the only other reported example is a small float in a river in northern Dominican Republic (Hattori *et al.* 2009). The presence of garnet-bearing peridotite in the Sanbagawa belt shows that this region preserves rocks exhumed from unusually deep within an oceanic-type subduction zone: greater

*Correspondence.

†Present address: Department of Earth Sciences, Kanazawa University, Kanazawa 920-1192, Japan.

Received 22 November 2008; accepted for publication 6 August 2009.

doi:10.1111/j.1440-1738.2009.00696.x

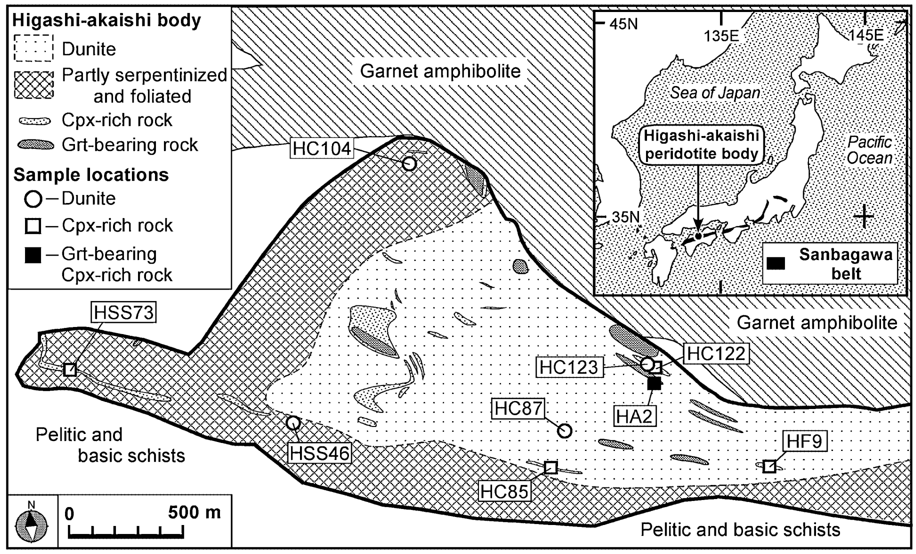

Fig. 1 Sampling locations. Distribution of the Sanbagawa belt and the study area are shown in the insert.

than 100 km (Enami *et al.* 2004). In addition, the Higashi-akaishi body is well-exposed and provides an exceptional opportunity to study deep-seated subduction processes without the extensive metamorphic overprint common in continental collisional zones. Furthermore, these rocks have potential importance in understanding the evolution of the eastern margin of the Asian continent.

The metamorphic history of the Higashi-akaishi ultramafic rocks is now well-established (Enami *et al.* 2004; Mizukami & Wallis 2005), but their protolith is contentious. Many workers have assumed a lower crustal cumulate origin (e.g. Kunugiza *et al.* 1986; Kunugiza & Takasu 2002). However, Mizukami *et al.* (2004) suggest that it was derived from the mantle wedge above the subduction plate. A third view presented by Terabayashi *et al.* (2005) suggests that adjacent gabbroic bodies and sedimentary rocks formed together with the Higashi-akaishi peridotites and that the sequence represents the remnants of a subducted oceanic plateau. In their proposed model, the oceanic plateau was transported northwestward by the oceanic lithosphere to the eastern margin of the Asian continent before subduction in the Sanbagawa subduction zone. This paper tests these hypotheses using geochemical data to establish the protolith of these rocks. We conclude that it represents part of a root of an arc with important implications for solid-state flow in the mantle wedge in the Cretaceous eastern Asian margin.

GEOLOGICAL SETTING

The Sanbagawa belt dominantly consists of basic and pelitic schists with lesser amounts of quartz-rich schists. The metamorphic grade generally increases toward the northern boundary, the Median Tectonic Line (Fig. 1). Ultramafic and gabbroic rocks are volumetrically small but with their associated metasedimentary rocks they include the most deeply subducted part of the Sanbagawa accretionary complex (e.g. Takasu 1989; Enami *et al.* 2004).

The largest of the ultramafic bodies, the Higashi-akaishi body, occurs as a coherent but relatively thin (≤300 m) sheet close to the highest structural level in the belt (Mizukami & Wallis 2005). Its outer margin is in contact with pelitic and basic schists and has been sheared and hydrated, but large parts preserve relatively anhydrous ultramafic rocks that consist of olivine and pyroxene (Mori & Banno 1973; Mizukami & Wallis 2005). Field and microscopic observations suggest that the outer margins of the body contain significant amounts of serpentine, but the interior is mostly anhydrous (Fig. 1). The values of loss on ignition (LOI) are less than 3.5 wt%, which may be compared to values greater than 13 wt% for serpentinites. Therefore, the Higashi-akaishi ultramafic body cannot be described as a serpentinite body. Other ultramafic rocks in the Sanbagawa belt form small lenses with less than 1 km in exposed length, which have been hydrated to form serpentinites (e.g. Kunugiza *et al.* 1986). Garnet has not been identified from these small serpentinite lenses.

LITHOLOGY AND MINERALOGY OF HIGASHI-AKAISHI BODY

Previous workers classified the rocks in the Higashi-akaishi body into different units based on fabrics and textures (e.g. Bamba 1953; Yoshino 1964). In this paper, we classify them into two rock types: olivine-dominated rocks (dunite, minor harzburgite) and minor clinopyroxene-rich rocks (clinopyroxenite, minor wehrlite and websterite). Olivine-dominated rocks are predominantly dunite (Mori & Banno 1973). Orthopyroxene is extremely rare in the Higashi-akaishi body and only occurs in its northern part. Therefore, orthopyroxene-bearing rocks, such as websterite and harzburgite, are also restricted to the northern part. Among them, harzburgite is very rare. Mori and Banno (1973) reported that harzburgite forms lenses in the northern part of the Higashi-akaishi body and the Jiyoshi ultramafic body, which is located north of the Higashi-akaishi body separated by the quartz–kyanite eclogite unit. These workers also described dykes of harzburgite injecting into epidote amphibolite schist near the Higashi-akaishi body. Due to intense deformation and alteration associated with harzburgites and the ambiguous contact relationships between harzburgite and other rock units of the Higashi-akaishi body, the origin of the harzburgite and the relationship between harzburgite and dunite are not certain. Considering the rare occurrence of harzburgite, we did not study this rock type.

Dunite consists of olivine with minor chromite and antigorite. Antigorite forms well-crystalline blades of up to 1 mm in length. It cross-cuts olivine grains and occurs along grain boundaries. The microstructure of a typical partially serpentinized and foliated dunite is shown in figure 3e of Mizukami and Wallis (2005). Chromite occurs as euhedral to subhedral grains of up to 4 mm in size. It is commonly rimmed by ferritchromite and Cr-bearing magnetite (<20 μm in width in most grains). The cores are homogeneous in composition and those of different grains show similar compositions in individual thin-sections. Such core compositions are considered to be primary and used in this study.

Garnet is very rare in olivine-dominated rocks. It occurs only in the tectonized northern part of the Higashi-akaishi body where lenticular clinopyroxene-rich rocks are abundant. Although garnet is in contact with olivine, garnet is clearly associated with clinopyroxene in hand specimen and outcrop scales. Garnet occurs as euhedral to subhedral grains, and elongated grains along grain boundaries of other minerals. Garnet commonly contains mineral inclusions, and photomicrographs showing inclusions of olivine and chromite in garnet appear in the articles of Mizukami and Wallis (2005) and Enami *et al.* (2004). The texture and occurrence of garnet suggest that garnet has grown at a relatively late stage in olivine-dominated rocks.

Clinopyroxene-rich rocks in the Higashi-akaishi body are clinopyroxenite, wehrlite, and websterite. They are easily identified in the field because pale green clinopyroxene stands out on the weathered surface of rocks. Clinopyroxene-rich rocks form boudins, layers, and irregular veins of several millimeters to meters in thickness within dunite. The clinopyroxene-rich rocks contain minor olivine, garnet, amphiboles, and oxides. In contrast to homogeneous and monomineralic dunite, clinopyroxene-rich rocks show heterogeneous modal abundance on length scales of less than 1 cm. They commonly contain monomineralic bands and layers, as shown in the photograph of Tsujimori *et al.* (2000). Garnet forms large euhedral crystals, up to 2 mm, tabular and elongated grains along grain boundaries of other minerals. Coarse garnet grains commonly contain inclusions of other minerals. Inclusions of amphiboles, chlorite, and magnetite have been reported in garnet in clinopyroxenite by Enami *et al.* (2004). The mineral compositions of clinopyroxene-rich rocks are reported by Mori and Banno (1973), Enami *et al.* (2004), and Mizukami and Wallis (2005).

Chromite-rich lenses and bands occur in dunite in the north and eastern part of the Higashi-akaishi body, and were once extracted as refractory material (Bamba 1953; Mori & Banno 1973). The boundaries are sharp in hand specimen but gradational in outcrop scales (Yoshino 1961). Boundaries consist of varying proportions of chromite and olivine that is completely replaced by serpentine (Bamba 1953). The occurrence of kaemmerite, Cr-rich chlorite, is reported in association with chromite-rich layers (Mori & Banno 1973).

SAMPLES

The samples used in this study are representative rock types of the Higashi-akaishi body and were selected after careful mapping and petrographic examination. They are dunite (HC87, HC104, HC123, HSS46, HSS73), wehrlite (HC85, HC122, HF9), and garnet websterite (HA2); their locations are shown in Figure 1. The dunite sample HC87 contains thin (<1 mm in width) chromitite seams and the sample HSS73 contains a clinopyroxenite veinlet of less than 1 mm in width. Sample HC87 is the least hydrated dunite with well-preserved olivine grains. The dunite is composed of olivine with minor antigorite, chromite, and magnetite. Careful examination of thin-sections of all samples did not reveal the presence of any sulphide grains in our olivine-dominated samples.

Clinopyroxene-rich samples contain olivine with minor garnet, oxides, amphibole, and chlorite. The abundance of minerals vary widely even within hand specimens. Chromite occurs in HC85, HC122, and HF9. Clinopyroxene forms similar-sized grains, up to 2 mm in HC85. All chromite grains are small and extensively oxidized to ferritchromite and Cr-magnetite, but several grains retain cores with Cr-spinel composition. Oxides are commonly associated with small angular grains of pentlandite and Ni-bearing pyrrhotite, but spherical or globular grains of sulphides are not found in the studied samples. Sample HA2 contains monomineralic orthopyroxene-rich and garnet-rich layers (~1 cm in width) and a photograph of the hand specimen is shown in figure 5b of Tsujimori *et al.* (2000). Enami *et al.* (2004) used this sample for their thermobarometric study and reported the mineralogy, texture, and mineral chemistry of the sample in their paper.

ANALYTICAL METHODS

The concentrations of major and minor elements in bulk rocks were determined on fused disks with an X-ray fluorescent spectrometer. Trace elements were determined with an inductively coupled plasma-mass spectrometer (HP-4500, Agilent Technologies, Tokyo, Japan) after HF–HNO_3 digestion. Contents of platinum group elements (PGE) were determined by isotopic dilution method using a mixed spike of ^{99}Ru, ^{105}Pd, ^{190}Os, ^{191}Ir, and ^{194}Pt after pre-concentration of PGE into a Ni–sulphide button. Typical blanks were 0.002–0.006 ng Ru/g flux, 0.002–0.008 ng Ir/g flux, 0.002–0.006 ng Os/g flux, 0.07–12 ng Pt/g flux and 0.03–1 ng Pd/g flux. The analytical procedure is described in Hattori and Guillot (2007).

Mineral compositions were determined using a JXA-8900R electron microprobe (JEOL, Tokyo, Japan) in wavelength dispersive mode at Nagoya University. Analytical conditions are a 15 kV accelerating voltage, about 12 nA beam current in the Faraday cup, and a beam diameter of 2–3 μm. Raw data were corrected using the *ZAF* method. The contents of Fe^{3+} in spinel were calculated assuming spinel stoichiometry.

RESULTS

BULK COMPOSITIONS

Dunite contains high concentrations of all compatible elements, such as Cr (>3000 ppm), Ni (>1800 ppm), and MgO (>43 wt%) (Table 1). Most contain low concentrations of moderately incompatible elements, such as Al_2O_3 (<0.5 wt%) and TiO_2 (<0.05 wt%), compared to abyssal peridotites (Fig. 2a). Sample HC123 contains slightly elevated Al_2O_3 (1.2 wt%), TiO_2 (0.14 wt%), MnO (0.21 wt%), and total Fe (11.6 wt% as Fe_2O_3) due to the presence of chromitite seams, but these concentrations are still low compared to the primitive mantle compositions of McDonough and Sun (1995). Furthermore, these dunite samples contain high concentrations of Ir-type PGE, such as Os, Ir and Ru (Fig. 3). As Ir-type PGE remain in mantle residues during partial melting (e.g. Righter *et al.* 2004; Brenan *et al.* 2005), high Ir-type PGE concentrations suggest that these rocks are likely to be refractory mantle peridotites.

Clinopyroxene-rich rocks contain high concentrations of fluid-mobile elements (i.e. Sr, Ba) relative to high field strength elements (Nb, Y, Zr, Ti), and show a characteristic concentration pattern of elements known as a ‘subduction-related geochemical signature’ (Fig. 2b). The moderately incompatible elements, such as Al and Y, are overall higher than dunite samples and compatible elements are low compared to dunite. For example, the contents of Ni are lower than 1000 ppm, and those of Cr below 3000 ppm except for HC122, which contains coarse chromite grains. The data suggest that these rocks likely represent ultramafic cumulates of basaltic magmas. Their cumulate origin is further supported by low concentrations of Ir-type PGE (Fig. 3), as they are retained in the residue during partial melting.

MINERAL CHEMISTRY

Spinel

Cores of chromite grains show similar compositions among different grains in individual samples (Fig. 4b). They have low Y_{Fe3+} (= Fe^{3+}/[Al + Cr + Fe^{3+}] < 0.17), TiO_2 (<0.4 wt%), V_2O_3 (<0.2 wt%), and ZnO (<0.5 wt%), and are characterized by low Mg# (= Mg/[Mg + Fe^{2+}] = 0.31–0.46) and high Cr# (= Cr/[Cr + Al] > 0.7) (Fig. 4a,b). The compositions are similar to those of chromite in the Mariana forearc peridotites (Ishii *et al.*

Table 1 Bulk rock compositions

lithology			HA2 webs	HC85 wehr	HC122 wehr	HF9 wehr	HC87 dunite	HC104 dunite	HC123 dunite	HSS46 dunite	HSS73 dunite
SiO_2	%	XRF	52.2	49.6	43.3	44.1	38.5	40.4	37.0	38.6	42.1
TiO_2	%	XRF	0.12	0.045	0.11	0.041	0.04	0.02	0.14	0.02	0.02
Al_2O_3	%	XRF	2.05	0.62	1.82	0.63	0.46	0.26	1.21	0.23	0.22
CaO	%	XRF	16.2	16.6	9.32	8.86	0.49	0.48	0.45	0.43	3.49
MgO	%	XRF	19.5	23.1	30.5	33.1	47.3	44.1	44.0	44.7	43.2
Fe_2O_3t	%	XRF	8.19	5.86	11.5	7.78	7.21	7.29	11.6	8.72	8.38
MnO	%	XRF	0.14	0.12	0.19	0.16	0.11	0.11	0.21	0.13	0.13
P_2O_5	%	XRF	0.01	0.01	0.02	0.01	0.02	0.01	0.02	0.01	0.01
LOI	%	XRF	0.5	2.8	2.6	4.4	7.1	8.8	3.8	8.3	2.5
sum		XRF	98.9	98.7	98.9	99.0	101.2	101.4	98.5	101.1	100
Cr	ppm	XRF	1080	2640	3810	2570	9990	3750	69 500	3130	3590
Ni	ppm	XRF	221	171	825	468	2360	2030	2 320	2100	1790
V	ppm	XRF	239	69	104	34	14	22	147	17	14
Co	ppm	XRF	46	51	99	95	107	105	149	116	107
Zn	ppm	ICP	12	10	35	19	9.5	15	9.4	23	20
Ba	ppm	ICP	13	4.1	5.4	3	3.1	3	3.2	1.2	3.4
Ce	ppm	ICP	8.7	0.3	4.2	0.3	0.2	0.2	0.6	0.0	0.2
Nb	ppm	ICP	0.16	0.07	0.37	0.06	0.08	0.07	0.28	0.07	0.05
Nd	ppm	ICP	5	0.2	2.7	0.3	0.1	0.1	0.4	<0.1	0.2
Rb	ppm	ICP	0.4	0.2	0.6	0.2	0.1	0.1	0.1	0.1	0.1
Sr	ppm	ICP	140	16	77	13	4	4	2	1	31
Y	ppm	ICP	2.1	0.5	2.1	0.7	0.1	0.1	0.2	<0.05	0.5
Zr	ppm	ICP	2.8	0.2	1.7	0.4	0.5	0.3	0.5	0.1	0.2
Sc	ppm	ICP	73.3	45.1	40.9	26	4.2	5.7	2.6	4.1	14.4
Pb	ppm	ICP	2.63	0.92	0.54	0.37	0.14	0.12	0.45	0.10	0.19
Os	ppb	ICP	0.13	0.23	0.33	0.31	1.14	4.22	2.23	2.43	3.08
Ir	ppb	ICP	0.04	0.41	0.42	0.05	0.70	3.76	1.41	0.95	2.98
Ru	ppb	ICP	0.17	0.41	1.33	1.43	3.54	6.88	5.43	1.82	4.28
Pt	ppb	ICP	106	44.1	39.0	8.97	0.26	6.04	1.68	0.60	15.4
Pd	ppb	ICP	300	5.19	70.2	2.68	1.40	0.58	2.20	0.45	14.9
Mg#			0.825	0.886	0.840	0.894	0.928	0.923	0.883	0.910	0.911

Fe_2O_3t, total Fe expressed as Fe_2O_3; webs, websterite; wehr, wehrlite; Mg#, atomic ratios of Mg/(Mg + Fe).
ICP, inductively coupled plasma mass-spectrometry; LOI, loss on ignition; ppb; parts per billion; ppm, parts per million; XRF, X-ray fluorescence spectrometer.

1992) and other forearc mantle peridotites (e.g. Arai & Ishimaru 2008). Our spinel displays distinctly higher Cr# than those observed in abyssal peridotites (e.g. Dick & Bullen 1984), and oceanic islands (Barnes & Roeder 2001). Chromite in abyssal peridotites and oceanic islands rarely shows the values Cr# exceeding 0.6.

Spinel grains in clinopyroxene-rich rocks (samples HC85, HC122, HF9) show a wide compositional variation with increasing Fe^{3+} and TiO_2 towards rims. Cores of spinel grains in sample HF9 have similar compositions among different grains with low Fe^{3+} ($Y_{Fe3+} < 0.20$) and moderately high Cr# (~0.60) (Figs 4a,b,5). They are considered to be primary and plotted in the diagrams (Fig. 4a,b).

Olivine

In dunite, olivine has a high forsterite content (Fo = 100 × Mg/[Mg + Fe]), ranging from 90 to 94.5, whereas the values range from 81 to 88 in clinopyroxene-rich rocks. The composition of olivine obtained in this study is very similar to those reported from the Higashi-akaishi body by previous workers (e.g. Kunugiza 1980). For example, Mori and Banno (1973) also found high Fo values (~93) in dunite and harzburgite and lower Fo values (83–92) in clinopyroxene-rich rocks. The NiO contents of olivine show a broad positive correlation with Fo values and range from 0.28 to 0.48 wt% in olivine-dominated rocks and from 0.08 to 0.26 wt% in clinopyroxene-rich rocks (Fig. 4c). Both NiO and Fo values plot in the field for mantle peridotites, but slightly higher than the fertile spinel–garnet lherzolites (Fig. 4c). The values are distinctly higher than those of abyssal peridotites (Dick 1989; Sobolev *et al.* 2005). Olivine in highly refractory abyssal peridotites still contains Fo values up to 92 (Seyler *et al.* 2007). The data from the Higashi-akaishi body suggest that

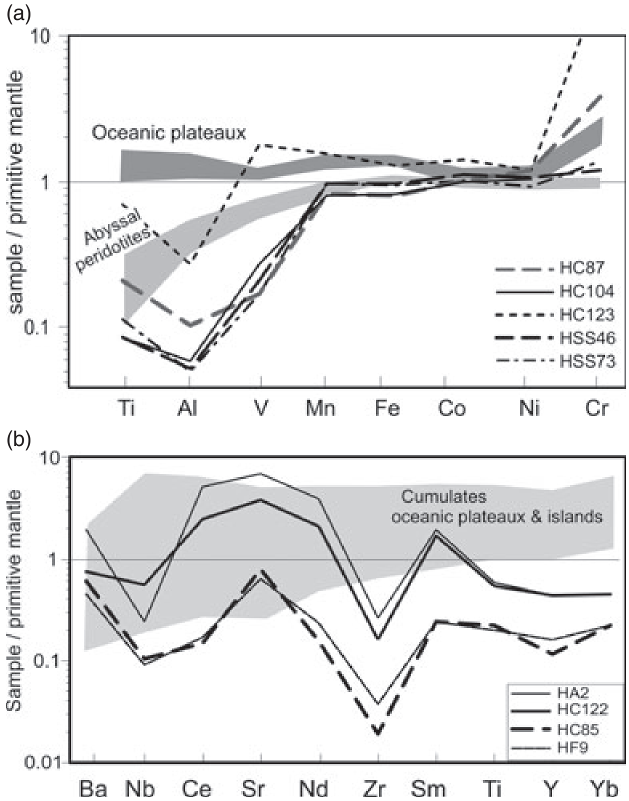

Fig. 2 Primitive mantle-normalized bulk chemical compositions of (a) olivine-dominated ultramafic rocks, and (b) clinopyroxene-rich rocks. Primitive mantle values are after McDonough and Sun (1995). The values of abyssal peridotites are lower and upper quartile values for 124 abyssal peridotites in Niu, (2004). Cumulates of oceanic plateau are clinopyroxene-rich ultramafic from the base of Drakkarpo unit, an accreted oceanic island in the Himalayas (Guillot *et al.* 2000), clinopyroxenites from the Bolívar Complex, an accreted oceanic plateau in Colombia (Kerr *et al.* 2004), and dunites and wehrlite from Gorgona Island, Colombia (Révillon *et al.* 2000). Dunites from Gorgona Islands have low values.

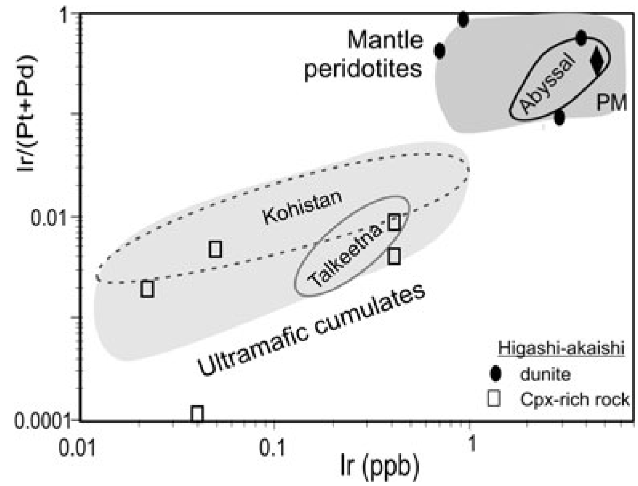

Fig. 3 Iridium and Ir/(Pt + Pd) w/w ratios of bulk rocks, showing the primitive mantle value (◆). The field for mantle peridotites includes abyssal peridotites (Rehkämper *et al.* 1999), Horoman, Japan (Rehkämper *et al.* 1999), Zabargad, Red Sea, Ronda, Spain, and forearc mantle serpentinites in Himalayas (Guillot *et al.* 2000). The field for ultramafic cumulates includes data from the Jijal ultramafic complex of the Kohistan Arc, Pakistan, and Talkeetna Arc (Guillot *et al.* 2000). Note that olivine-dominated rocks contain high Ir and plot in the field for mantle peridotites, whereas clinopyroxene-rich rocks are in the field for cumulates.

olivine-dominated rocks originated from highly refractory mantle peridotites. This is also consistent with their plot in the olivine–spinel mantle array of Arai (1994). The compositions of our olivine and spinel from dunite plot in the refractory peridotites (Fig. 5).

Olivine in clinopyroxene-rich rocks contains low and varying MgO and NiO compared to that in olivine-dominated rocks (Fig. 4c). Olivine compositions plot a broad curve expected during the fractional crystallization of a mafic melt (Fig. 4c). The data suggest that they are likely cumulates of a mafic melt. Nickel is a chalcophile as well as lithophile and it would be preferentially incorporated in a sulphide liquid when the melt is saturated in S. The broad correlation between Fo and NiO values suggests that the parental melt for clinopyroxene-rich rocks was not saturated with S and that sulphide content was insignificant during the crystallization of olivine. The compositions of olivine and spinel from sample HF9 plot outside the olivine–spinel mantle array of Arai (1994) (Fig. 5).

Mori and Banno (1973) suggested silicate minerals have undergone subsolidus re-equilibration based on broad positive correlations between Fe and Mg among different minerals and high values of apparent Fe–Mg partition coefficients. Olivine in clinopyroxene-rich rocks would have acquired reduced Mg/(Mg + Fe) during the subsolidus equilibration, but no change is expected in NiO. The observed relationship between NiO and Mg/(M + Fe) (Fig. 4c) suggest that the change in Mg, if there was any, was minor.

Clinopyroxene

Clinopyroxene is diopsidic and contains high MgO, low TiO_2, and low Na_2O (Mori & Banno 1973; Enami *et al.* 2004). As has been pointed out, diopsidic clinopyroxene in the Higashi-akaishi body differs from metamorphic pyroxene formed in eclogites. Clinopyroxene in our samples contains low Al_2O_3 compared to that in alkaline igneous rocks (Le Bas 1962; Fig. 4d). The contents of Al is

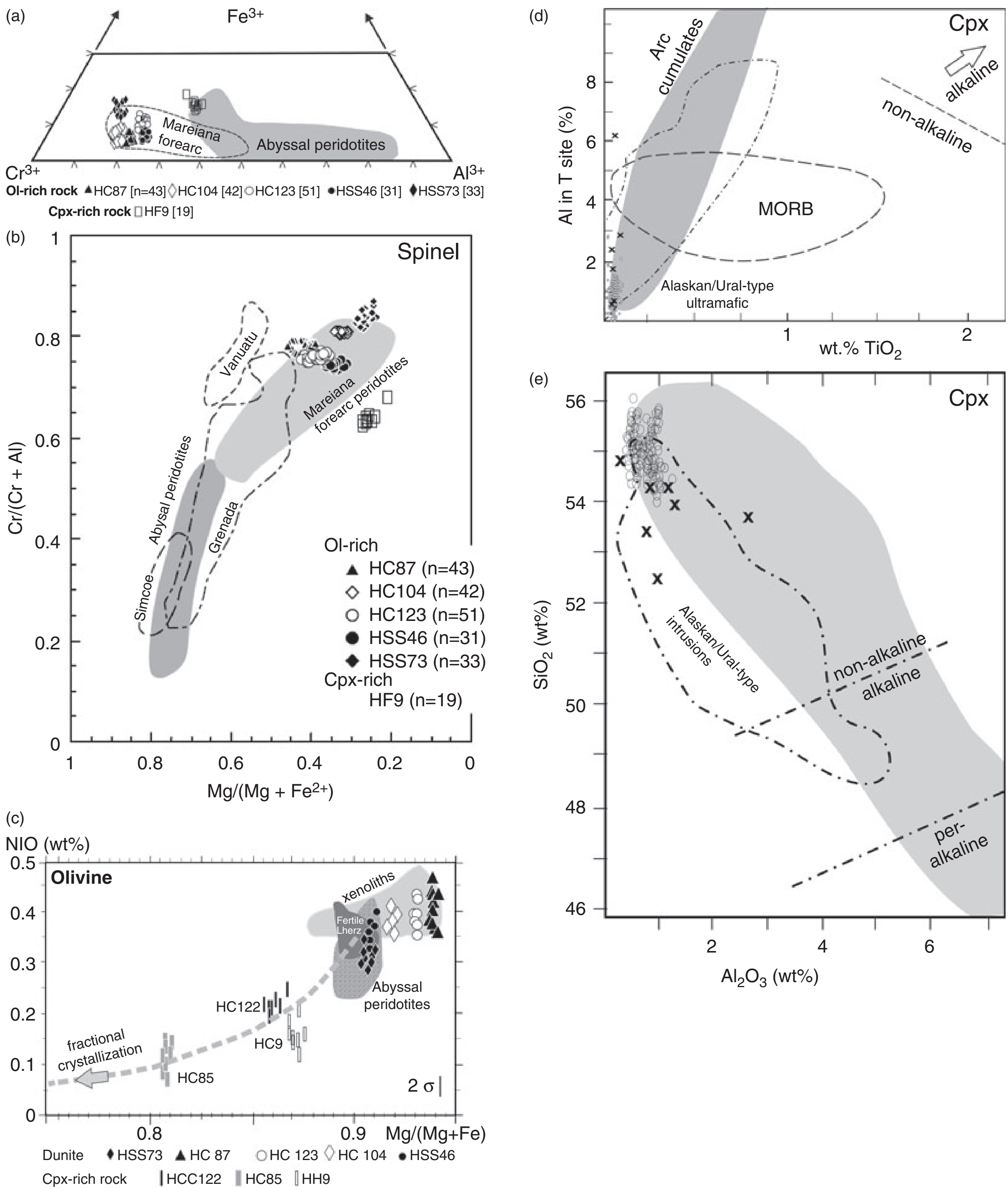

mostly less than 2% in the tetrahedral site of clinopyroxene, which makes our clinopyroxene distinct from those in mid-oceanic ridge basalts and in alkaline igneous rocks common in oceanic plateaux and islands. Clinopyroxene in the Higashi-akaishi ultramafic rocks plots in the field of arc cumulates in the SiO_2–Al_2O_3 discrimination diagram of Loucks (1990) (Fig. 4e).

Fig. 4 (a,b) Compositions of spinel in the Higashi-akaishi ultramafic body compared to those of abyssal peridotites (Dick & Bullen 1984; Bonatti & Michael 1989), Mariana forearc peridotites (Ishii *et al.* 1992), peridotite xenoliths in primitive basalts in Vanuatu, Simcoe, and Grenada (Parkinson *et al.* 2003). Numbers of grains plotted are 42 for HC104, 51 for HC123, 43 for HC87, 31 for HSS46, 33 for HSS73, and 19 for HF9. Cores of spinel grains with $Y_{Fe3+} < 0.2$ are plotted. (c) Contents of NiO *vs* forsterite (Fo) values of olivine from the Higashi-akaishi ultramafic body. Light gray field of mantle peridotites is after Fleet *et al.* (1977), dark grey field is for lherzolite xenoliths in kimberlites (Sato 1977), darkest field is for fertile spinel–garnet lherzolite xenoliths in southern South America (Wang *et al.* 2008b), dark patterned field for most abyssal peridotites (e.g. Dick 1989; Sobolev *et al.* 2005). Thick gray arrow shows the compositional variation of olivine during fractional crystallization of mafic melt starting with 0.4 wt% NiO and Fo value of 90 (Sato 1977). The original values of Mg/(Mg + Fe) of olivine in clinopyroxene-rich rocks may be greater than that observed if olivine has undergone low-temperature equilibration with clinopyroxene, as suggested by Mori and Banno (1973). We consider that the modification of olivine composition was minor as the observed values of Ni and Mg plot on the expected fractionation curve. In addition, the low-temperature equilibration, ~700°C, may change Mg/(Mg + Fe) of olivine up to 0.04, considering the Mg–Fe exchange thermometry of Brey and Köhler (1990). (d,e) Compositions of clinopyroxene grains from the Higashi-akaishi body plotted in the clinopyroxene discrimination diagram of (d) Loucks (1990) and (e) LeBas (1962). Arc cumulate field is shown in gray. Dashed-dot and dashed areas are the fields for clinopyroxene composition of the Phanerozoic subduction-related Alaskan/Ural-type ultramafic-mafic intrusions (Helmy & El Mahallawi 2003; Pettigrew & Hattori 2006) and the Archaean subduction-related ultramafic-mafic intrusions in the Quetico belt (Pettigrew & Hattori 2006). Compositions of clinopyroxene grains in Enami *et al.* (2004) including those in sample HA2 (○); and those presented in Mori and Banno (1973) (×).

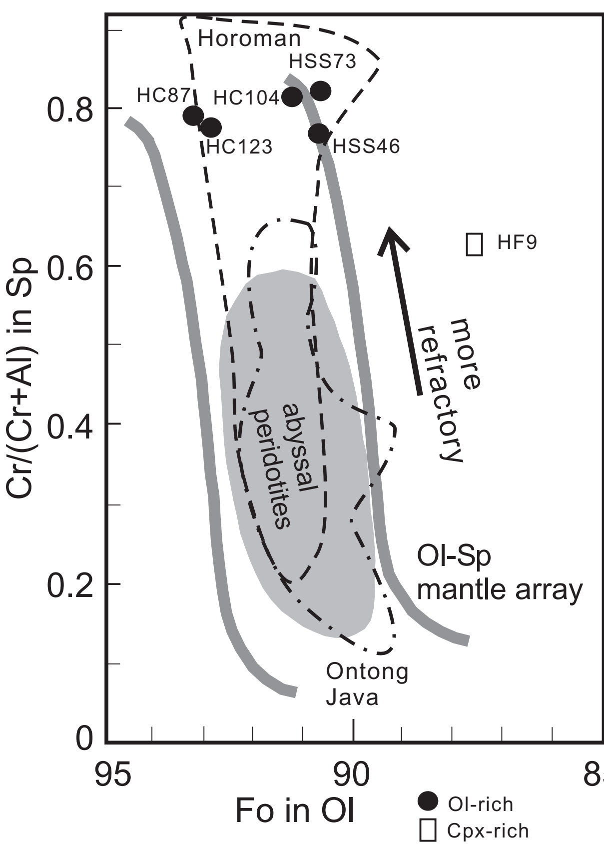

Fig. 5 Forsterite component of olivine *vs* Cr# of spinel. The compositional range of mantle peridotites (Ol–Sp mantle array) and abyssal peridotites are from Arai (1994), Horoman peridotites in Japan from Takazawa (1996) and Takahashi (1991), and peridotites underlying the Ontong Java Plateau from Ishikawa *et al.* (2004). Note that clinopyroxene-rich sample (HF9) does not plot in the mantle array.

DISCUSSION

ORIGIN OF ULTRAMAFIC ROCKS

Clinopyroxene-rich rocks

Bulk compositions of clinopyroxene-rich rocks show relatively low concentrations of Ir-type PGE compared to the primitive mantle composition (Fig. 3). These elements have high partition coefficients (*D*) between mantle minerals and melt (e.g. Puchtel & Humayun 2001; Righter *et al.* 2004) and remain in the residual mantle during partial melting. The *D*-values for these elements are particularly high in oxides. Considering the occurrences of oxides in clinopyroxene-rich rocks, the low concentrations of Ir-type PGE suggest that these rocks are not residual mantle rocks. Instead, they are ultramafic cumulates of melts.

A cumulate origin of these rocks is further supported by overall low contents of Ni and Cr in bulk rock samples (Table 1). They are compatible with mantle minerals and also tend to remain in the residual mantle. Clinopyroxene-rich rocks show low Nb and Zr compared to rare earth elements, which produce a fractionated primitive mantle-normalized pattern (Fig. 2b). The element pattern can not be explained by solidification processes because crystallization of olivine and clinopyroxene in varying proportions does not separate these elements. Therefore, the pattern reflects that of the original melt and the source mantle and implies that the source mantle for the parental melt had been enriched in these fluid-mobile elements. The geochemical data combined with the geological setting suggest that clinopyroxene-rich rocks are most likely cumulates of a subduction-related melt.

The interpretation is consistent with the compositions of olivine, clinopyroxene, and spinel. As described above, the compositions of olivine and spinel do not fall within the field for mantle peridotites, olivine–spinel mantle array of Arai (1994) (Fig. 5).

Clinopyroxene contains low Al and plots in the arc cumulate field (Fig. 4d,e). Olivine shows overall low contents of Ni and Mg (Fig. 4c). Both Mg and

Ni contents are too low to be considered residual mantle peridotites. The broad positive correlation between Ni and Mg in olivine suggests that the parental melt was not saturated with S to form a sulphide liquid because Ni together with PGE would be preferentially partitioned into the sulphide liquid (e.g. Fleet *et al.* 1977, 1996). These rocks therefore formed as cumulates from sulphur-poor magmas.

Olivine-dominated rocks

There are several possible origins of olivine-dominated rocks: (i) cumulate of mafic melt; (ii) metasomatic product; and (iii) residue after extensive partial melting. The Higashi-akaishi ultramafic body contains chromitite layers in dunites. As dunites commonly occur as cumulates with chromitite layers, it has been proposed that the Higashi-akaishi ultramafic body is a cumulate of a mafic melt (e.g. Kunugiza 1980). The cumulate origin of dunite in the Higashi-akaishi body appears to be supported by minor abundance of dunite in mantle xenoliths. However, the low abundance of dunites in subarc mantle xenoliths does not imply the paucity of highly refractory dunite residue in mantle. Most subarc mantle xenoliths are brought to the surface by explosive alkaline volcanic rocks in back-arcs. Peridotites in back-arcs are fertile compared to forearc mantle peridotites as shown by the variation in Cr# of spinel and Mg# of silicate minerals. In fact, the occurrences of refractory dunites are common as the protoliths of forearc mantle serpentinites (e.g. Ishii *et al.* 1992; Parkinson & Pearce 1998). More importantly, the lithology of xenoliths is likely biased towards more fertile peridotites (e.g. Griffin *et al.* 2008) because the mantle peridotites are likely affected by the melt before the volcanism that brings xenoliths to the surface. Therefore, highly refractory dunites may be more common in the upper mantle than previously considered (e.g. Bernstein *et al.* 2007; Griffin *et al.* 2008).

The bulk rock geochemical data and mineral chemistry of our olivine-dominated rocks are consistent with their cumulate origin. The concentrations of Ir-type PGE are high in olivine-dominated rocks (Table 1, Fig. 3). These elements have high partition coefficients between mantle minerals and melt. For example, D-values for Ru and Ir between spinel and melt are greater than 100 and those between olivine and melt greater than 1 (e.g. Puchtel & Humayun 2001; Righter *et al.* 2004). Therefore, a partial melt in the upper mantle should show low concentrations of Ir-type PGE. In theory, early-formed spinel could contain significant concentrations of Ir-type PGE, but the crystallization of a small quantity of spinel would remove much of PGE from the melt. Therefore, ultramafic cumulates even in the upper mantle contain variable but low concentrations of Ir-type PGE (e.g. Wang *et al.* 2008b).

High concentrations of PGE in our dunite could be related to the formation of sulphides. However, this is not applicable to the samples studied. After careful examination, we did not find any sulphides in the dunite samples. It may be further argued that sulphides were later removed from the rocks. We discount this possibility because overall high contents of Ni and Mg in olivine in our samples (Fig. 4c) suggest that S was insignificant in our samples. It may be further argued that dunites were enriched in PGE during later hydrothermal alteration and/or metamorphism. We reject this possibility because PGE, especially Ir-type PGE, are known to be immobile during high-temperature alteration and metasomatism. For example, highly metasomatized rocks, such as orthopyroxenite formed from harzburgite, retain the original PGE contents (e.g. Wang *et al.* 2008b). In addition, crustal rocks contain low concentrations of Ir-type PGE (e.g. McLennan 2001). Therefore, high concentrations of PGE in dunites can not be explained by their introduction during the exhumation. Consistently high concentrations of all Ir-type PGE in our samples suggest that the rocks are most likely residual mantle peridotites (Fig. 3).

The residual mantle origin is further supported by consistently high Mg and Ni in olivine (Fig. 4c) and high Cr# of chromite in dunites (Fig. 4a,b). The contents of Mg and Ni in our olivine samples are even higher than those of fertile lherzolites (Fig. 4c). Spinel in dunite samples shows high Cr# (Fig. 4d). Spinel in cumulates commonly shows a wide range of Cr# (Barnes & Roeder 2001) because Cr content rapidly decreases in a melt whereas Al remains in the melt. This is not observed in the Higashi-akaishi samples.

The remaining possible origin of dunite is a metasomatic product. Dunites may be formed as a metasomatic product of harzburgite through a reaction with a hydrous mafic melt (Kelemen 1990). This possibility is not supported by high Mg in our olivine samples. Olivine in metasomatized rocks commonly shows variable Mg content after reacting with a mafic melt (e.g. Wang *et al.* 2008b). Therefore, dunites formed from harzburgites contain low Mg olivine (e.g. Morgan & Liang 2003). Furthermore, the metasomatic origin is not supported by the textures of dunite in the Higashi-akaishi body. Dunite bodies formed by metasomatism commonly contain remnants of pre-metasomatic rocks and reaction zones between them (e.g. Quick 1981). There is no evidence supporting the existence of pre-metasomatic rock in the Higashi-akaishi body.

We suggest that our dunite represents refractory peridotite formed as the result of high degrees of partial melting after influx fusion of clinopyroxene and later of orthopyroxene (e.g. Kubo 2002; Bernstein *et al.* 2007) in the mantle wedge. The proposed interpretation is further supported by the abundance of highly refractory dunite as for the xenoliths of Mesozoic igneous rocks in eastern China (e.g. Xu *et al.* 2008). Mantle xenoliths are mostly spinel-bearing dunite with very minor harzburgite. The evidence suggests that the northeastern margin of the Asian continent was mostly underlain by refractory dunite.

ORIGINAL SITE OF HIGASHI-AKAISHI ULTRAMAFIC BODY

The highly refractory geochemical characteristics of the Higashi-akaishi peridotites suggest their original site in the mantle wedge. Refractory mantle peridotites may also occur in the oceanic lithosphere, but abyssal peridotites are not as refractory as peridotites in a mantle wedge. The compilation of 128 bulk rock compositions of abyssal peridotites by Niu (2004) shows that the median value of Al_2O_3 is 1.94 wt%. Our samples contain even lower Al_2O_3 (1.2 wt%) than the lower quartile value (1.36 wt%) of abyssal peridotites (Fig. 2a), suggesting that olivine-dominated rocks are much more refractory than abyssal peridotites. This is further confirmed by the compositions of olivine and Cr-spinel. As described above, even highly refractory dunite and harzburgite of abyssal peridotite show Fo values less than 92 (e.g. Seyler *et al.* 2007). The values of Cr#, greater than 0.7, in our Cr-spinel are greater than those of abyssal peridotites (Fig. 4a,b). The Cr# for spinel in abyssal peridotites rarely reaches 0.60 (Dick & Bullen 1984).

Our olivine-dominated rocks are too refractory to be considered in association with oceanic islands or plateaux (Fig. 2a). Mantle plumes producing oceanic islands and plateaux are fertile as they ascend from the deep mantle. Refractory peridotites may possibly be produced in the shallow mantle overlying a plume head due to extensive partial melting induced by the hot plume, but highly refractory peridotites similar to our samples have not been reported from oceanic plateaux or islands. Volcanic rocks of oceanic plateaux and islands do not show a severe depletion of incompatible elements, which suggests that such refractory mantle peridotites are not likely to be found beneath oceanic plateaux and islands. Rare occurrences of mantle peridotites associated with plumes and plateaux are relatively fertile with low Cr# in spinel, mostly less than 0.6 (e.g. Barnes & Roeder 2001; Ishikawa *et al.* 2004; Fig. 5). A further argument against an oceanic island or plateau origin comes from the TiO_2 content. Chromite from oceanic plateaux and islands commonly contains significantly high TiO_2, greater than 1.0 wt%, reflecting the fertile nature of the source mantle (Kamenetsky *et al.* 2001), which is in contrast with consistently low TiO_2, <0.4 wt%, in our chromite. We therefore discount the possibility that our olivine-dominated rocks originated as part of an oceanic plateau or island sequence.

The presence of clinopyroxene-rich cumulate rocks in the Higashi-akaishi body suggests that the ultramafic body was in a site where melt percolated through. This is further supported by the occurrence of chromite-rich bands and layers in dunite in the Higashi-akaishi body. Chromite-rich bands in peridotites are generally interpreted as the reaction products of residual mantle peridotites with mafic melt along their conduits (e.g. Arai & Yurimoto 1994; Valfalvy *et al*. 1996).

There are two possible locations in the mantle wedge to satisfy this condition: forearc and subarc mantle. We suggest that the Higashi-akaishi body was likely present in the forearc mantle based on several lines of evidence. First, a short distance is required for forearc mantle peridotites to be incorporated in the subduction channel (Fig. 6b). Second, forearc mantle peridotites are more refractory than subarc mantle peridotites, as shown by high Cr in spinel and high Mg in silicate minerals (Figs 4b,5). Our samples plot in the forearc mantle peridotite field (Fig. 5). Furthermore, the subduction of the Higashi-akaishi body most likely took place during an early stage of the subduction system, judging from the anticlockwise pressure–temperature (P–T) path of the metamorphism (Enami *et al.* 2004; Mizukami & Wallis 2005; Fig. 6). The anticlockwise burial P–T path recorded in the Higashi-akaishi (Mizukami & Wallis 2005) suggests that the subduction zone was in the initial stage of subduction where thermal steady state had not been reached (e.g. Krogh

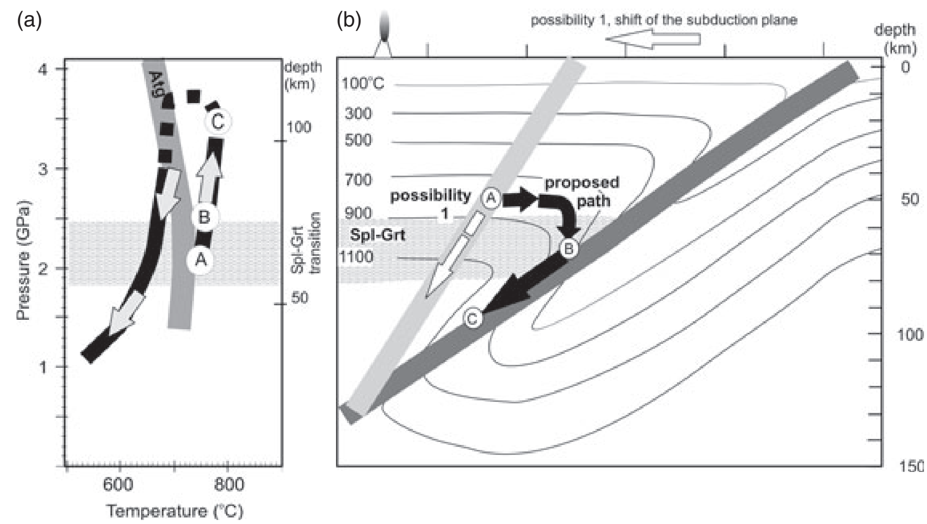

Fig. 6 (a) Pressure–temperature path of the Higashi-akaishi body, and (b) schematic vertical section of the Sanbagawa subduction zone showing the path of the body. *P–T* path is primarily based on the work by Enami *et al.* (2004) and Mizukami and Wallis (2005). Positions A, B, and C are defined based on the core and rim compositions of garnet and orthopyroxene (Enami *et al.* 2004). The position of garnet–spinel (Grt–Spl) transition (dotted area) is after the occurrences of spinel and garnet peridotites by O'Neil (1981) and Wang *et al.* (2008a). We use the antigorite (Atg) stability limit of Ulmer and Trommsdorff (1995), which is at higher temperatures than other workers, but this may be applicable to natural samples as the presence of Al increases the stability limit (Bromley & Pawley 2003). Possible paths of the Higashi-akaishi ultramafic body are shown in the schematic vertical section of the subduction zone. Temperature contours are based on the numerical model of Gerya *et al.* (2002) where a 40-my-old oceanic plate is subducted for 0.6 my at an angle of 60° and a rate of 15 cm/yr. A, B and C correspond to positions in the pressure–temperature diagram of (a). The thick white arrow shows possible movement of the Higashi-akaishi body if the subduction plane shifted towards the arc (possibility 1). Thick solid arrows show the proposed movement of the body where the Higashi-akaishi body was dragged to the subduction channel.

et al. 1994). Numerical modeling by Uehara and Aoya (2005) suggests that thermal steady state is attained in less than 10 my in an oceanic subduction zone with a subduction rate of 10 cm/year. The Sanbagawa metamorphism was associated with subduction of the Izanagi Plate (Wallis *et al.* 2009), which moved at around 20 cm/year (Engebretson *et al.* 1985). The rapid subduction rate would result in more rapid approach to a thermal steady state than given above.

Forearc magmatism is common in the 'infant' stage of subduction as the initiation of subduction likely produces a local rift in the forearc, an upwelling of hot asthenospheric mantle, and the formation of boninitic magmas (e.g. Jonathan & Jacobi 2002; Lissenberg *et al.* 2005). The situation may be applicable to the Higashi-akaishi body.

Enami *et al.* (2004) estimated the pressures of the Higashi-akaishi body based on the compositions of orthopyroxene and garnet. The core compositions yielded approximately 1.5–2.4 GPa and 700–800°C and rim compositions 2.9–3.8 GPa and 700–810°C (Fig. 6a). The *P–T* condition estimated from the rims corresponds to depths of 100–120 km in the subduction channel with a geotherm of about 7°C/km. The *P–T* condition estimated from the core compositions correspond to a depth of 40–70 km. The depth is within the spinel–garnet transition zone of fertile peridotites (O'Neil 1981), but the transition zone is dependent on bulk compositions, as the stability field of spinel increases with increasing Cr in bulk rocks (Klemme 2004). Considering that our samples contain high Cr and low Al, the *P–T* condition of the Higashi-akaishi body estimated from the core compositions likely corresponds to that in the spinel peridotite field of the upper mantle (Fig. 6b). This implies that garnet likely formed later during high-pressure metamorphism along the subduction channel.

TRANSPORTATION OF HIGASHI-AKAISHI BODY

It has been suggested that ultramafic bodies in the belt protruded into the upper crustal level as serpentinite diapirs (e.g. Takasu 1989), based on the occurrences of small serpentinite lenses in the Sanbagawa belt and abundant serpentinite diapirs in the Mariana forearc. We discount this possibility. If the Higashi-akaishi body was once a serpentinite unit, it had to be later dehydrated to become an essentially anhydrous body. Such rocks should show distinct features. For example, olivine transformed from serpentine minerals contains abundant inclusions of fluids, magnetite, and serpentine (e.g. Trommsdorff & Evans 1980). Magnetite inclusions are not present in our samples. Furthermore, metamorphic olivine commonly contains high Mg and low Ni, reflecting the composition of serpentine (e.g. Kunugiza 1980; Hattori & Guillot 2007). Olivine in our samples plots in the mantle peridotite field (Fig. 4c). In addition this possibility is not consistent with the *P–T* path recorded in the Higashi-akaishi rocks (Fig. 6a; Enami *et al.* 2004). The increase in pressure recorded in the rocks is best explained by its incorporation in the subduction channel (Fig. 6b).

Incorporation of the Higashi-akaishi body in the Sanbagawa subduction channel is supported by the metamorphic *P–T* path of the Higashi-akaishi body, which shows a minor cooling before a sharp increase in pressures reaching about 3 GPa in the subduction channel (Fig. 6a; Enami *et al.* 2004). This is consistent with the horizontal movement of the body towards the trench (Fig. 6b).

The incorporation of the ultramafic body into the subduction channel requires either propagation of the subduction boundary towards a pre-existing arc (possibility 1 in Fig. 6b), or a strong horizontal flow towards the trench in the mantle wedge (Fig. 6b). It is difficult to achieve the observed *P–T* path during the propagation of the subduction plate (possibility 1) as the wedge mantle is hotter farther away from the subduction plate (Fig. 6b). Therefore, we suggest that the Higashi-akaishi body was transported towards the subduction channel by an active mantle flow. This proposed interpretation is supported by several lines of evidence listed below.

POSSIBLE CAUSE FOR STRONG ACTIVE MANTLE FLOW

A mantle flow is induced by the subduction of a slab and it would be stronger in a subduction zone that lacks a lubricating layer along the interface between two converging plates. There are two possible lubricants for a subduction plane: sediments at shallow depths and serpentinites at deeper levels (e.g. Guillot *et al.* 2001). They are absent in the initial stage of subduction. Thus, an active mantle flow is expected in this stage.

Furthermore, the Sanbagawa subduction channel was hotter than many oceanic-type subduction zones during the subduction of the Higashi-akaishi body (Mizukami & Wallis 2005) and remained on the high temperature side of the stability field of antigorite (Fig. 6a). The lack of serpentinites likely produced an ill-lubricated interface between the overlying mantle wedge and the subducting slab, which produces a stronger corner flow in the overlying mantle wedge.

As mentioned earlier, garnet-bearing peridotites are very rare in oceanic-type subduction zones and the only other reported example is in the northern Dominican Republic (Abbott *et al.* 2006). This area has voluminous serpentinites (Saumur *et al.* 2009) and the exhumation of garnet-bearing peridotites is attributed to the formation of a wide serpentinite-rich subduction channel and the weakened mantle wedge by extensive hydration (Gorczyk *et al.* 2007). This condition is not applicable to the Sanbagawa belt during the subduction of the Higashi-akaishi body.

The presence of such a large body of garnet-bearing peridotite in the Sanbagawa belt requires an exceptional condition that was not fulfilled in other oceanic-type subduction zones. We propose that the regional tectonic setting likely contributed to this exceptional condition. The formation of the Sanbagawa belt coincided with a major mantle overturning event in northeastern Asia. The northeastern Asian continent had been stable since late Archaean (e.g. Zhai 2004) and underlain by a thick (~250 km) stable lithospheric mantle that was composed of highly refractory peridotites. This cold lithospheric mantle was replaced by hot asthenospheric mantle in Jurassic to Cretaceous time (e.g. Griffin *et al.* 1998; Gao *et al.* 2002). The ascent of the hot asthenospheric mantle resulted in extensive igneous activity in northern China (e.g. Wu *et al.* 2005) and thinning of the lithospheric mantle to about 60–70 km (e.g. Griffin *et al.* 1998; Deng *et al.* 2007). The voluminous hot asthenospheric mantle had to dissipate by moving eastward along the base of the lithosphere at a depth of approximately 65 km because it was blocked by deep roots of the Yangtze craton to the south, the Mongolian block to the west, and the Aldan Shield to the north. This major eastward flow of hot asthenospheric mantle likely contributed to a stronger mantle flow in the eastern margin of Asia and may have contributed to keeping the wedge mantle hotter than usual.

CONCLUSIONS

Bulk rock and mineral compositions suggest that dunite is a refractory mantle residue after extensive partial melting, and that clinopyroxene-rich rocks are cumulates of a subduction-related melt.

They were originally in the shallow mantle wedge in the spinel peridotite field, and entrained in a mantle flow before being incorporated into the Sanbagawa subduction channel and subducted to a depth of greater than 100 km. The occurrence of the garnet-bearing peridotite in the Higashi-akaishi body reflects the exceptional conditions of the Sanbagawa subduction zone, which is rarely attained in other oceanic-type subduction zones. A strong mantle flow was produced in the mantle wedge due to the poor development of lubricants along the interface between two plates. It was unusually hot and this prevented the formation of lubricating serpentinite. The high temperatures probably reflect conditions at an early stage in the development of the Sanbagawa subduction system and this would therefore lack wet accreted sediments that could also act as a lubricant. In addition, the Higashi-akaishi subduction also coincides with the time of massive upwelling of the asthenospheric mantle in the eastern margin of the Asian continent. Eastward flow of the host asthenospheric mantle likely contributed to the hot temperatures and strong mantle flow in the area.

ACKNOWLEDGEMENTS

The authors thank M. Wilk-Alemany and R. Hartree for analysis of bulk rock samples at the University of Ottawa. KH thanks Nagoya University for a Visiting Professorship in the fall of 2008 to conduct this research. The project was supported by a Discovery Grant to KH from the Natural Science and Engineering Research Council of Canada, and grants to ME and SW from the Japan Society for Promotion of Science (Nos. 18340172, 19654080, 19540503). Comments from S. Arai and E. Takazawa (Associate Editor) were helpful in clarifying the manuscript.

REFERENCES

ABBOTT R. N. JR., DRAPER G. & BROMAN B. N. 2006. P-T path for ultrahigh-pressure garnet ultramafic rocks of the Cuaba Gneiss, Rio San Juan Complex, Dominican Republic. *International Geology Review* 48, 778–90.

ARAI S. 1994. Characterization of spinel peridotites by olivine-spinel compositional relationships: review and interpretation. *Chemical Geology* **111**, 191–204.

ARAI S. & ISHIMARU S. 2008. Insights in petrological characteristics of the lithosphere of mantle wedge beneath arcs through peridotite xenoliths: a review. *Journal of Petrology* **49**, 665–95.

ARAI S. & YURIMOTO H. 1994. Podiform chromitites of the Tari-Misaka ultramafic complex, southwestern Japan, as mantle-melt interaction products. *Economic Geology* **89**, 1219–88.

BAMBA T. 1953. The Higashi Akaishi-yama dunite mass in Shikoku (Studies on spinels associated with the ultramafic rocks, II). *Journal of Geological Society of Japan* **59**, 437–45 (in Japanese with English Abstract).

BARNES S. J. & ROEDER P. L. 2001. The range of spinel compositions in terrestrial mafic and ultramafic rocks. *Journal of Petrology* **42**, 2279–302.

BERNSTEIN, S., KELEMEN, P. B. & HANGHØJ, K. 2007. Consistent olivine Mg# in cratonic mantle reflects Archean mantle melting to the exhaustion of orthopyroxene. *Geology* **35**, 459–62.

BONATTI E. & MICHAEL P. J. 1989. Mantle peridotites from continental rifts to ocean basins to subduction zones. *Earth and Planetary Science Letters* **91**, 297–311.

BRENAN J. M., MCDONOUGH W. F. & ASH R. 2005. An experimental study of the solubility and partitioning of iridium, osmium and gold between olivine and silicate melt. *Earth and Planetary Science Letters* **237**, 855–72.

BREY G. P. & KÖHLER T. 1990. Geothermobarometry in four-phase lherzolites II. New Thermobarometers, and practical assessment of existing thermobarometers. *Journal of Petrology* **31**, 1353–78.

BROMLEY G. D. & PAWLEY A. R. 2003. The stability of antigorite in the systems $MgO-SiO_2-H_2O$ (MSH) and $MgO-Al_2O_3-SiO_2-H_2O$ (MASH): the effects of Al^{3+} substitution on high-pressure stability. *American Mineralogist* 88, 99–108.

BRUECKNER H. K. & MEDARIS L. G. 2000. A general model for the intrusion and evolution of 'mantle' garnet peridotites in high-pressure and ultra-high-pressure metamorphic terranes. *Journal of Metamorphic Geology* 18, 123–33.

DENG J., SU S., NIU Y. *et al.* 2007. A possible model for the lithospheric thinning of North China Craton: evidence from the Yanshanian (Jura-Cretaceous) magmatism and tectonism. *Lithos* **96**, 22–35.

DICK H. H. J. B. 1989. Abyssal peridotites, very slow spreading ridges and ocean ridge magmatism. *In* Saunders A. D., Norry M. J. (eds.) *Magmatism in the Ocean Basins*. Geological Society, London, Special Publication **42**, pp. 71–105.

DICK H. J. B. & BULLEN T. 1984, Chromian spinel as a petrogenetic indicator in abyssal and alpine-type peridotites and spatially associated lavas. *Contributions to Mineralogy and Petrology* **86**, 54–76.

ENGEBRETSON D. C., COX A. & GORDON R. G. 1985. Relative motions between oceanic ad continental plates in the Pacific basin. *Geological Society of America Special Paper* **206**, 1–59.

ENAMI M., MIZUKAMI T. & YOKOYAMA K. 2004. Metamorphic evolution of garnet-bearing ultramafic rocks from the Gongen area, Sanbagawa belt, Japan. *Journal of Metamorphic Geology* **22**, 1–15.

FLEET M. E., CROCKET J. H. & STONE W. E. 1996. Partitioning of platinum group elements (Os, Ir, Ru, Pt, Pd) and gold between sulfide liquid and basalt melt. *Geochimica et Cosmochimica Acta* **60**, 2397–2412.

FLEET M. E., MACRAE N. D. & HERZBERG C. T. 1977. Partition of nickel between olivine and sulfides: a test for immiscible sulfide liquids. *Contributions to Mineralogy and Petrology* **65**, 191–7.

GAO S., RUDNICK R. L., CARLSON R. W. *et al.* 2002. Re-Os evidence for replacement of ancient mantle lithosphere beneath the North China craton. *Earth and Planetary Science Letters* **198**, 307–22.

GERYA T., STÖCKHERT B. & PERCHUK A. L. 2002. Exhumation of high-pressure metamorphic rocks in a subduction channel: a numerical simulation. *Tectonics* **21**, 1056, doi:10.1029/2002TC001406.

GORCZYK W., GUILLOT S., GERYA T. V. & HATTORI K. H. 2007. Asthenospheric upwelling, oceanic slab retreat and exhumation of UHP mantle rocks: insights from Greater Antilles. *Geophysical Research Letters* **34**, L 21309. doi:10.1029/2007GL031059

GRIFFIN W. L., O'REILLY S. Y., AFONSO J. C. & BEGG G. C. 2008. The composition and evolution of lithospheric mantle: a re-evaluation and its tectonic implications. *Journal of Petrology* doi:10.1093/petrology/egn033

GRIFFIN W. L., ZHANG A., O'REILLY S. Y. & RYAN C. G. 1998. Phanerozoic evolution of the lithosphere beneath the Sino-Korean craton. *In* Flower M. *et al. Mantle Dynamics and Plate Interactions in East Asia*. American Geophysical Union, Washington, D.C., Geodynamics Series **27**, 107–26.

GUILLOT S., HATTORI K. H. & DE SIGOYER, J. 2000. Mantle wedge serpentinization and exhumation of eclogites: insights from eastern Ladakh, NW Himalaya. *Geology* 28, 199–202.

GUILLOT S., HATTORI K., DE SIGOYER J., NÄGLER T. & AUZENDE A. L. 2001. Evidence of hydration of the mantle wedge and its role in the exhumation of eclogites. *Earth and Planetary Science Letters* **193**, 115–27.

HATTORI K. H. & GUILLOT S. 2007. Geochemical character of serpentinites associated with high- to ultrahigh-pressure metamorphic rocks in the Alps, Cuba, and the Himalayas: recycling of elements in subduction zones. *Geochemistry Geophysics and Geosystems* 8, Q09010, doi:10.1029/2007GC001594.

HATTORI K., GUILLOT S., SAUMUR B-M., TUBRETT M. N., VIDAL O. & MORFIN S. 2009. Corundum-bearing garnet peridotite from northern Dominican Republic: A metamorphic product of an arc cumulate in the Caribbean subduction zone, *Lithos*, doi:10.1016/j.lithos.2009.10.010.

HELMY H. M. & EL MAHALLAWI M. M. 2003. Gabbro Akarem mafic-ultramafic complex, Eastern Desert, Egypt: a late Precambrian analogue of Alaskan-type Complexes. *Mineralogy and Petrology* **77**, 85–108.

ISHIKAWA A., MARUYAMA S. & KOMIYA T. 2004. Layered lithospheric mantle beneath the Ontong Java Plateau: implications from xenoliths in Alnöite, Malaia, Solomon Islands. *Journal of Petrology* **45**, 2011–44.

ISHII T., ROBINSON P. T., MAEKAWA H. & FISKE R. 1992. Petrological studies of peridotites from diapiric serpentinites seamounts in the Izu-Ogasawara-Mariana forearc, Leg 125. *In* Fryer P., Pearce J. A., Stokking L. B., *et al. Proc. ODP., Scientific Results, 125*. Ocean Drilling Program, College Station, TX. **125**, 445–85. doi:10.2973/odp.proc.sr.125.129.1992

ISOZAKI Y. & ITAYA T. 1990. Chronology of Sambagawa metamorphism. *Journal of Metamorphic Geology* **8**, 401–11.

JONATHAN K. & JACOBI R. D. 2002. Boninites: characteristics and tectonic constraints, northeastern Appalachians. *Physics and Chemistry of the Earth* **27**, 109–47.

KAMENETSKY V. S., CRAWFORD A. J. & MEFERE S. 2001. Factors controlling chemistry of magmatic spinel: an empirical study of associated olivine, Cr-spinel and melt inclusions from primitive rocks. *Journal of Petrology* **42**, 655–71.

KELEMEN P. B. 1990. Reaction between ultramafic rock and fractionating basaltic magma I. Phase relations, the origin of calc-alkaline magma series, and the formation of discordant dunite. *Journal of Petrology* **31**, 51–98.

KERR A. C., TARNEY J., KEMPTON P. D. *et al.* 2004. Mafic pegmatites intruding oceanic plateau gabbros and ultramafic cumulates from Bolívar, Colombia: evidence for a 'wet' mantle plume? *Journal of Petrology* **45**, 1877–906.

KLEMME S. 2004. The influence of Cr on the garnet–spinel transition in the Earth's mantle: experiments in the system $MgO–Cr_2O_3–SiO_2$ and thermodynamic modelling. *Lithos* **77**, 639–46.

KROGH E., OH C. W. & LIOU G. 1994. Polyphase and anticlockwise *P-T* evolution for Franciscan eclogites and blueschists from Jenner, California, USA. *Journal of Metamorphic Geology* **12**, 121–34.

KUBO K. 2002. Dunite formation processes in highly depleted peridotite: case study of the Iwanaidake peridotite, Hokkaido, Japan. *Journal of Petrology* **43**, 423–48.

KUNUGIZA K. 1980. Dunites and serpentinites in the Sanbagawa metamorphic belt, central Shikoku and Kii peninsula, Japan. *Journal of Japan Association of Mineralogy, Petrology, Economic Geology* **75**, 14–20.

KUNUGIZA K., TAKASU A. & BANNO S. 1986. The origin and metamorphic history of the ultramafic and metagabbro bodies in the Sanbagawa metamorphic belt. *Geological Society of America Memoir* **164**, 375–85.

KUNUGIZA K. & TAKASU A. 2002. Geology of the Western Iratsu mass within the tectonic mélange zone in the Sambagawa metamorphic belt, Besshi district, central Shikoku, Japan. *Journal of the Geological Society of Japan* **108**, 644–62.

LE BAS M. J. 1962. The role of aluminum in igneous clinopyroxenes with relation to their parentage. *American Journal of Science* **260**, 267–88.

LISSENBERG C. J., VAN STAAL C. R., BÉDARD J. H. & ZAGOREVSKI A. 2005. Geochemical constraints on the origin of the Annieopsquotch ophiolite belt, Newfoundland Appalachians. *Geological Society of America Bulletin* **117**, 1413–26.

LOUCKS R. R. 1990. Discrimination of ophiolitic from nonophiolitic ultramafic-mafic allochthons in orogenic belt by the Al/Ti ratio in clinopyroxene. *Geology* **18**, 346–9.

MCDONOUGH W. & SUN S. S. 1995. The composition of the earth. *Chemical Geology* **120**, 223–53.

MCLENNAN S. M. 2001. Relationships between the trace element composition of sedimentary rocks and upper continental crust. *Geochemistry, Geophysics, Geosystems* **2**, 1021, doi:10.1029/2000GC000109.

MIZUKAMI T. & WALLIS S. R. 2005. Structural and petrological constraints on the tectonic evolution of the garnet-lherzolite facies Higashi-akaishi peridotite body, Sanbagawa belt, SW Japan. *Tectonics* **24**, doi:10.1029/2004TC001733.

MIZUKAMI T., WALLIS S. R. & YAMAMOTO J. 2004. Natural examples of olivine lattice preferred orientation patterns with a flow-normal a-axis maximum. *Nature* **427**, 432–6.

MORGAN Z. & LIANG Y. 2003. An experimental and numerical study of the kinetics of harzburgite reactive dissolution with applications to dunite dike formation. *Earth and Planetary Science Letters* **214**, 59–74.

MORI T. & BANNO S. 1973. Petrology of peridotite and garnet clinopyroxenite of the Mt. Higashi-Akaishi mass, Central Shikoku, Japan – Subsolidus relation of anhydrous phases. *Contributions to Mineralogy and Petrology* **41**, 301–23.

NIU Y. 2004. Bulk-rock major and trace element compositions of abyssal peridotites: implications for mantle melting, melt extraction and post-melting processes beneath mid-ocean ridges. *Journal of Petrology* **45**, 2423–58.

O'NEIL H. St C. 1981. The transition between spinel lherzolite and garnet lherzolite, and its use as a geobarometer. *Contributions to Mineralogy and Petrology* **77**, 185–94.

PARKINSON I. J. & PEARCE J. A., 1998. Peridotites from the Izu–Bonin–Mariana Forearc (ODP Leg 125): evidence for Mantle Melting and Melt–Mantle Interaction in a Supra-Subduction Zone Setting. *Journal of Petrology* **39**, 1577–618.

PARKINSON I. J., ARCULUS R. J. & EGGINS S. M. 2003, Peridotite xenoliths from Grenada, Lesser Antilles Island Arc. *Contributions to Mineralogy and Petrology* **146**, 241–62.

PETTIGREW N. T. & HATTORI K. H. 2006. The Quetico Intrusions of Western Superior Province: Neo-Archean examples of Alaskan/Ural-type mafic-ultramafic intrusions. *Precambrian Research* **149**, 21–42.

PUCHTEL I. S. & HUMAYUN M. 2001. Platinum group element fractionation in a komatiitic basalt lava lake. *Geochimica et Cosmochimica Acta* **65**, 2979–93.

QUICK J. E. 1981. The origin and significance of large, tabular dunite bodies in the Trinity peridotite, northern California. *Contributions to Mineralogy and Petrology* **78**, 413–22.

REHKÄMPER M., HALLIDAY A. N., ALT J. *et al.* 1999. Non-chondritic platinum-group element ratios in oceanic mantle lithosphere: petrogenetic signature of melt percolation? *Earth and Planetary Science Letters* **172**, 65–81.

RÉVILLON S., ARNDT N. T., CHAUVEL C. & HALLOT E. 2000. Geochemical study of ultramafic volcanic and plutonic rocks from Gorgona Island Colombia: the plumbing system of an oceanic plateau. *Journal of Petrology* **41**, 1127–53.

RIGHTER K., CAMPBELL A. J., HUMAYUN M. & HERVIG R. L. 2004. Partitioning of Ru, Rh, Pd, Re, Ir, and Au between Cr-bearing spinel, olivine, pyroxene and silicate melts. *Geochimica et Cosmochimica Acta* **68**, 867–80.

SATO H. 1977. Nickel content of basaltic magmas: identification of primary magmas and a measure of the degree of olivine fractionation. *Lithos* **10**, 113–20.

SAUMUR B.-M., HATTORI K. H. & GUILLOT S. 2009. Contrasting origins of serpentinites in the northern Dominican Republic. *Geological Society of America Bulletin*. doi: 10.1130/B26530.1, Data Repository 2009134

SEYLER M., LORAND J. P., DICK H. D. B. & DROUIN M. 2007. Pervasive melt percolation reactions in ultra-depleted refractory harzburgites at the Mid-Atlantic Ridge, 15–20°N: ODP Hole 1274A. *Contributions to Mineralogy and Petrology* **153**, 303–19.

SOBOLEV A. V., HOFMANN A. W., SOBOLEV S. V. & NIKOGOSIAN I. K. 2005. An olivine-free mantle source of Hawaiian shield basalts. *Nature* **434**, 590–7.

TAKAHASHI N. 1991. Evolutional history of the uppermost mantle of an arc system: Petrology of the Horoman Peridotite Massif, Japan. *In* Nicolas A. & Coleman R. G. (eds.) *Ophiolite Genesis and Evolution of the Ocean Lithosphere*. pp. 195–205, Kluwer, Dordrecht.

TAKASU A. 1989. P-T histories of peridotite and amphibolite tectonic blocks in the Sanbagawa metamorphic belt, Japan. *In* Daly J. S., Cliff R. A. & Yardley B. W. D. (eds.) *Evolution of Metamorphic Belts*. Geological Society, London, Special Publication **43**, pp. 533–38.

TAKAZAWA E. 1996. *Geodynamic Evolution of the Horoman Peridotite, Japan: Geochemical Study of Lithospheric and Asthenospheric Processes*. Ph. D. thesis, Massachusetts Institute of Technology, Boston.

TERABAYASHI M., OKAMOTO K., YAMAMOTO H. *et al.* 2005. Accretionary complex origin of the mafic-ultramafic bodies of the Sanbagawa Belt, central Shikoku, Japan. *International Geology Review* **47**, 1058–78.

TROMMSDORFF V. & EVANS B. W. 1980. Titanian hydroxyl-clinohumite: formation and breakdown in antigorite rocks (Malenco, Italy). *Contributions to Mineralogy and Petrology* **72**, 229–242.

TSUJIMORI T., TANAKA C., SAKURAI T. *et al.* 2000. Illustrated introduction to eclogite in Japan. *Bulletin of Research Institute of Natural Sciences, Okayama University of Science* **26**, 19–40.

UEHARA S. & AOYA M. 2005. Thermal model for approach of a spreading ridge to subduction zones and its implications for high-P/high-T metamorphism: importance of subduction versus ridge approach ratio. *Tectonics* 24 TC 4007. doi: 10.1029/2004TC001715.

ULMER P. & TROMMSDORFF V. 1995. Serpentine stability to mantle depths and subduction-related magmatism. *Science* **268**, 858–61.

VALFALVY V., HÉBERT R. & BEDARD J. H. 1996. Interactions between melt and upper mantle peridotites in the North Arm Mountain massif, Bay of Islands ophiolite, Newfoundland, Canada: implications for the genesis of boninitic and related magmas. *Chemical Geology* **129**, 71–90.

WALLIS S. R., ANCZKIEWICZ R., ENDO S., AOYA M., PLATT J. P., THIRLWALL M. & HIRATA T. 2009. Plate movements, ductile deformation ad geochronology of the Sanbagawa belt, SW Japan: tectonic significance of 89-88 Ma Lu-Hf eclogite ages. *Journal of Metamorphic Geology* **27**, 93–105.

WANG J., HATTORI K. H., LI J.-P. & STERN C. 2008a. Oxidation state of Paleozoic subcontinental lithospheric mantle below the Pali Aike volcanic field in southernmost Patagonia. *Lithos* **105**, 98–110.

WANG J., HATTORI K. H. & STERN C. 2008b. Metasomatic origin of garnet orthopyroxenites in the subcontinental lithospheric mantle underlying Pali Aike volcanic field, southern South America. *Mineralogy and Petrology* **94**, 243–58.

WU F. Y., LIN J. W., WILDE S. A., ZHANG X. O. & YANG J. H. 2005. Nature and significance of the Early Cretaceous giant igneous event in eastern China. *Earth and Planetary Science Letters* **233**, 103–19.

XU W., HERGT J. M., GAO S., PEI F., WANG W. & YANG D. 2008. Interaction of adakitic melt-peridotite: implications for the high-Mg# signature of Mesozoic adakitic rocks in the eastern North China craton. *Earth and Planetary Science Letters* **265**, 123–37.

YOSHINO G. 1961. Structural-petrological studies of peridotite and associated rocks of the Higashi-akaishi-yama district, Shikoku, Japan. *Journal of Science, Hiroshima University Section C* **3**, 343–402.

YOSHINO G. 1964. Ultramafic mass in the Higashi-Akaishi yama district, southwest Japan. *Journal of Science, Hiroshima University Section C* **4**, 333–64.

ZHAI M. 2004. Precambrian tectonic evolution of the North China Craton. *In* Malpas J., Fletcher C. J. N., Ali J. R. & Aitchison J. C. (eds.) *Aspects of the Tectonic Evolution of China*. Geological Society, London, Special Publications, **226**, 57–72.